Mitochondrial Sulfide Detoxification Requires a Functional Isoform O-Acetylserine(thiol)lyase C in *Arabidopsis thaliana*

Consolación Álvarez, Irene García, Luis C. Romero and Cecilia Gotor

Instituto de Bioquímica Vegetal y Fotosíntesis, Consejo Superior de Investigaciones Científicas y Universidad de Sevilla, Avda. Américo Vespucio, 49, 41092 Sevilla, Spain.

Running title: Functionality of OAS-C

Author for correspondence: Cecilia Gotor: gotor@ibvf.csic.es. Tel: 34.954489516. Fax: 34.954460065.

ABSTRACT

In non-cyanogenic species, the main source of cyanide derives from ethylene and camalexin biosyntheses. In mitochondria, cyanide is a potent inhibitor of the cytochrome c oxidase and is metabolised by the β-Cyanoalanine synthase CYS-C1, catalysing the conversion of cysteine and cyanide to hydrogen sulfide and β-cyanoalanine. The hydrogen sulfide released also inhibits the cytochrome c oxidase and needs to be detoxified by the O-acetylserine(thiol)lyase mitochondrial isoform, OAS-C, which catalyses the incorporation of sulfide to O-acetylserine to produce cysteine, thus generating a cyclic pathway in the mitochondria. The loss of functional OAS-C isoforms causes phenotypic characteristics very similar to the loss of the CYS-C1 enzyme, showing defects in root hair formation. Genetic complementation with the *OAS-C* gene rescues the impairment of root hair elongation restoring the wild type phenotype. The mitochondria compromise their capacity to proper detoxify cyanide and the resulting sulfide because the latter cannot re-assimilate into cysteine in the *oas-c* null mutant. Consequently, we observe an accumulation of sulfide and cyanide and of the alternative oxidase, which is unable to prevent the production of reactive oxygen species probably due to the accumulation of both toxic molecules. Our results allow us to suggest that the significance of OAS-C is related with its role in the proper sulfide and cyanide detoxification in mitochondria.

Keywords: Alternative oxidase*, Arabidopsis thaliana,* Cysteine, Cyanide, β-Cyanoalanine synthase, O-Acetylserine(thiol)lyase, Reactive oxygen species, Root hair, Sulfide

INTRODUCTION

Ethylene is involved in many aspects of the plant life cycle, including seed germination, root hair development, seedling growth, leaf and petal abscission, climacteric fruit ripening, organ senescence, and the modulation of plant responses to stresses. Ethylene is synthesized in the cytosol from methionine via S-adenosyl-L-methionine (AdoMet), which is first converted to 1-aminocyclopropane-1-carboxylic acid (ACC) catalyzed by the enzyme S-adenosyl-L-methionine methylthioadenosine-lyase (ACC synthase) and then ACC is converted to ethylene by the enzyme ACC oxidase (Bleecker and Kende, 2000). This second reaction generates equimolecular amounts of ethylene and cyanoformic acid, the latter of which is spontaneously degraded to carbon dioxide and cyanide (Peiser et al., 1984). In non-cyanogenic species, such as *Arabidopsis thaliana*, ethylene biosynthesis is the main source of cyanide. However, it has recently been demonstrated that the biosynthesis of camalexin, the characteristic phytoalexin of *A. thaliana*, is linked to cyanide formation. Therefore, during the biosynthesis of camalexin, the tryptophan-derived intermediate indole-3-acetonitrile is conjugated with cysteine to serve as substrate for the cytochrome P450 enzyme CYP71B15. This enzyme catalyzes the formation of the thiazoline ring as well as the release of cyanide and subsequent oxidative decarboxylation of dihydrocamalexic acid to camalexin (Bottcher et al., 2009). Therefore, under certain developmental or environmental conditions, plant cells produce significant amount of cyanide that may be harmful to those cells.

Cyanide is a phytotoxic molecule that potently inhibits many important metalloenzymes, such as Cu/Zn superoxide dismutase, catalase, nitrate and nitrite reductase, nitrogenase and peroxidases (Siegien and Bogatek, 2006). In mitochondria, cyanide is a potent inhibitor of cytochrome c oxidase, which is complex IV of the mitochondrial respiratory chain (Cooper and Brown, 2008). Therefore, cyanide accumulation must be prevented during an ethylene biosynthesis burst. The main cyanide detoxification process described in plants is the conversion of cyanide to β-cyanoalanine, which is converted to Asn, Asp and ammonia by NIT4 class nitrilases,

allowing the recycling of nitrogen (Piotrowski, 2008). Cyanide can also be detoxified to a lesser extent by thiosulfate sulfurtransferase (rhodanese) and mercaptopyruvate sulfurtransferase, which catalyses the transfer of sulfur ions from thiosulfate or mercaptopyruvate, respectively, to cyanide ions (Nakamura et al., 2000; Papenbrock and Schmidt, 2000; Papenbrock et al., 2011).

β-Cyanoalanine synthase (CAS) catalyses the conversion of cysteine and cyanide to hydrogen sulfide and β-cyanoalanine. In *A. thaliana*, the most abundant CAS enzyme, located in the mitochondria, is encoded by *CYS-C1* (At3g61440) (Hatzfeld et al., 2000; Yamaguchi et al., 2000), and contributes to most of the CAS activity in root and leaf tissues (Watanabe et al., 2008). The *Arabidopsis* CYS-C1 enzyme belongs to the β-substituted alanine synthase family that also comprises the three major O-acetylserine(thiol)lyase enzymes OAS-A1 (At4g14880), OAS-B (At2g43750) and OAS-C (At3g59760) (Watanabe et al., 2008), the L-cysteine desulfhydrase DES1 (At5g28030) (Alvarez et al., 2010) and the S-sulfocysteine synthase CS26 (At3g03630) (Bermudez et al., 2010). Phylogenetic analysis shows that the isoforms CYS-D1 and CYS-D2 are putative CAS enzymes (Jost et al., 2000); however, β-cyanoalanine synthase activity has not been observed *in vitro* for these enzymes (Hatzfeld et al., 2000; Yamaguchi et al., 2000).

Recently, the analysis of T-DNA insertional mutants defective in the CYS-C1 enzyme has demonstrated that mitochondrial CAS activity is essential to maintain a low level of cyanide for proper root hair development (Garcia et al., 2010).

Although cyanide is adequately detoxified in mitochondria through the formation of β-cyanoalanine, a co-product of the CAS enzymatic activity is hydrogen sulfide, which also inhibits oxygen consumption by inhibition of the mitochondrial cytochrome c oxidase. In mammalian systems, both HCN and H_2S are non-competitive inhibitors with respect to oxygen and show similar inhibition constants (Cooper and Brown, 2008). Therefore, the hydrogen sulfide produced by the detoxification of cyanide needs to be detoxified in the mitochondria by the mitochondrial isoform of the OASTL family. The mitochondrial enzyme OAS-C catalyses the incorporation of sulfide to O-acetylserine to produce cysteine, which in

turn could be used by CYS-C1 to detoxify cyanide, thus generating a cyclic pathway for cyanide detoxification in the mitochondria (Figure 1). The most highly expressed OASTL isoforms in *Arabidopsis* cells including OAS-C have been studied from the point of view of their involvement in the primary sulfate assimilation pathway and cysteine biosynthesis. Mitochondrial OAS-C contributes only 5% of total OASTL activity, but it has been suggested that OAS-C plays a much more important role than assumed (Heeg et al., 2008). Expression analysis has shown that OAS-C expression is higher in the roots than in the leaves and suggests that OAS-C plays a significant role in the roots (Watanabe et al., 2008).

In this work, our main goal has been to characterize in detail T-DNA-tagged OAS-C deficient mutants in relation to its possible role in the detoxification of sulfide and cyanide in *Arabidopsis* mitochondria, acting jointly with CYS-C1. We have confirmed the involvement of OAS-C in the maintenance of low levels of sulfide and cyanide in mitochondria.

RESULTS

Identification and Characterization of T-DNA Insertion Mutants Interrupting Different *Arabidopsis* OAS-C Gene Models

To deepen the understanding of the role of the OAS-C enzyme, we attempted the identification of new T-DNA insertion mutant alleles that are different from those previously described. Only one allele from the SALK collection, SALK_000860, has been previously characterized (Figure 2A) (Heeg et al., 2008; Watanabe et al., 2008). A screening of different T-DNA mutant collections revealed a different allele from the WiscDsLox T-DNA lines generated by Dr. Patrick Krysan and Dr. Sandra Austin-Phillips at the University of Wisconsin-Madison. The T-DNA insertion in this allele, WiscDsLox381A8, is located in the tenth intron of the *OAS-C* sequence that curiously is only present in the predicted *OAS-C* gene model one, whereas the T-

DNA insertion in the SALK allele is located in the first intron of the *OAS-C* sequence and consequently interrupts the three predicted splice variants (Figure 2A). We performed RT-PCR analysis of the kanamycin-resistant seedlings from the SALK_000860 line and isolated three different plants knockouts for the three *OAS-C* gene models. We also analyzed nine Basta and hygromycin-resistant seedlings from the WiscDsLox381A8 line, and four of them were knockouts for splice variant one and wild type for splice variants two and three (data not shown). One line of each T-DNA-tagged mutant was selected for real-time RT-PCR analysis using specific primers designed to discriminate between splice variant 1 and splice variants 2 and 3 (Supplemental Table 1). The results obtained corroborated the previous RT-PCR analysis (Figure 2B).

Biochemical characterization of both mutants showed that the intracellular Cys and glutathione contents in the leaves of the SALK_000860 mutant were similar to the values obtained in wild type leaves, but significant reductions of 30% of both cysteine and glutathione contents were observed in the roots as previously described (Heeg et al., 2008; Watanabe et al., 2008). However, the WiscDsLox381A8 mutant showed wild type levels of Cys and glutathione contents even in the roots (Table 1).

Moreover, we performed real-time RT-PCR on the OASTL gene family in the both mutants in leaf and root tissues. When compared with wild type, the transcript levels of the different gene members were identical in the WiscDsLox381A8 mutant, whereas in the both tissues we observed induction of *OAS-A1* and *OAS-B* gene expression in the SALK_000860 mutant, the latter being more significant, and repression of the three β-cyanoalanine synthase-like encoding genes *CYS-C1, CYS-D1* and *CYS-D2* (Figure 3).

Phenotypic Traits of the SALK_000860 Mutant Are Dependent on Growth Conditions

Phenotypic differences between both mutants and wild type were not observed in the aerial parts of the plants under normal long-day growth conditions either in soil or

solid MS medium. However, we could observe important differences in root tissues when grown on vertical MS medium without sucrose. There was appreciable that the roots of the SALK_000860 mutant showed shorter root hairs than either wild type or WiscDsLox381A8 mutant roots. This defect in hair root elongation in the SALK_000860 mutant was consistently observable in different batches of seedlings that were analyzed. Furthermore, genetic complementation of the mutant with the *OAS-C* gene resulted in wild type hair roots, thus confirming that the observed phenotype was indeed due to the mutation of the *OAS-C* gene (Figure 4). Due to the discrepancy of the *oas-c* mutant phenotype with previous reports (Heeg et al., 2008; Watanabe et al., 2008a), we explored the phenotype traits growing the seedlings in different media. When seedlings were grown on vertical MS medium with one-fourth strength of macronutrients phenotypic differences were observed. The whole seedlings of the SALK_000860 mutant showed a strong reduction in size when compared with either wild type or WiscDsLox381A8 mutant, and this defect was also rescued by *OAS-C* gene complementation (Figure 5). This growth phenotype was in agreement with previously reported smaller size of *oas-c* mutant lines (Heeg et al., 2008). When grown with sucrose in any of the growth media, nor shorter root hairs nor smaller seedlings were observable (Supplementary Figure 1 online).

The SALK_000860 Mutant Accumulates Cyanide and Sulfide

Because the root phenotype observed in the SALK_000860 mutant resembled that observed in the null *cys-c1* mutant (Garcia et al., 2010) and also showed the repression of the *CYS-C1* gene, we measured the total CAS activity in the leaf and root tissues. Compared with the activity levels in wild type plants, we determined a reduction in CAS activity of 15% in the leaves and a more significant reduction of 30% in the roots of the SALK_000860 mutant, while the WiscDsLox381A8 mutant showed wild type levels of CAS activity in both leaf and root tissues. Consistent with the reduction of CAS activity, there was a significant increase of cyanide in the SALK_000860 mutant, mainly in roots, which accumulated 25 % CN^- over the basal

levels of wild type (Table 2). We also measured the total level of sulfide and found a very significant increase of sulfide in leaves of the SALK_000860 mutant, which accumulated 76% more S^{2-}, and even a stronger increase in roots that showed 2-fold accumulation over the basal levels of wild type and WisDsLox381A8 mutant (Table 2).

The SALK_000860 Mutant Has Induced the Alternative Oxidase Pathway and the ROS Production

To determine if the measured cyanide accumulation in the SALK_000860 mutant lead to induction of the alternative oxidase pathway, we analyzed the expression level of the *AOX1a* gene in both *oas-c* mutants. The qRT-PCR showed a significant increase in *AOX1a* expression in the SALK_000860 mutant that was not observed in the WiscDsLox381A8 mutant compared to wild type (Figure 6).

We further measured the total respiration rates of leaf and root tissues and the proportions of the cytochrome and the alternative oxidase respiration pathways in the two mutants. We observed similar behavior in both the leaves and roots. Whereas the SALK_000860 mutant showed an induction of 50% in the respiration rate in the roots and slight and not significant increase in the leaves, the WiscDsLox381A8 mutant did not show significant differences in the respiration rates compared to wild type either in the leaves (92% of the wild type rate) or in the roots (94% of the wild type rate) (Figure 7). The increase in respiration of the SALK_000860 mutant was completely abolished even to rates below the rates of the wild type and the WiscDsLox381A8 mutant when SHAM, an inhibitor of the alternative oxidase pathway, was added (Figure 7).

Our results clearly show an induction of the alternative oxidase respiration pathway in the SALK_000860 mutant, probably as a protection to prevent over-reduction that can lead to excessive ROS production. Accordingly, we used the histochemical DAB method to examine the production of ROS in mature leaves of wild type and the two *oas-c* mutant plants. We clearly observed accumulation of

H_2O_2 in the SALK_000860 mutant leaves as a brown staining distributed along the leaf that was not present in the wild type and the WiscDsLox381A8 mutant leaves (Figure 8A). Furthermore, we quantified the amount of H_2O_2 in root tissues by spectrofluorimetry, and observed a significant increase of 25% in the concentration of H_2O_2 in the SALK_000860 mutant roots compared to wild type, whereas the amount of peroxide was not different in the WiscDsLox381A8 mutant (Figure 8B). Thus, the induction of alternative oxidase seems not to be sufficient to avoid the production of oxygen peroxide in the SALK_000860 mutant. Besides, the H_2O_2 detected in this mutant is signaled programmed cell death as we consistently observed lesions that are characteristic of spontaneous cell death in the leaves of the SALK_000860 mutant after staining with trypan blue that were not observed in the wild type or the WiscDsLox381A8 mutant (Figure 8C).

DISCUSSION

Several research groups have independently demonstrated in recent years that the cytosol is the most important compartment for cysteine synthesis in *Arabidopsis*. Free sulfide released from the plastids and OAS from the mitochondria are incorporated into Cys in the cytosol (Haas et al., 2008; Heeg et al., 2008; Watanabe et al., 2008; Watanabe et al., 2008b; Krueger et al., 2009). These results highlight the cytosolic OASTL isoform, OAS-A1, as the major contributor to Cys synthesis (Lopez-Martin et al., 2008). However, it is intriguing that the null *oas-c* mutant of the mitochondrial OAS-C, which contributes to 5% of the total OASTL activity, shows a growth phenotype when grown on soil under short-day conditions, which has been suggested is not linked to a limited capacity for Cys synthesis (Heeg et al., 2008). The presented results allow us to suggest that the significance of OAS-C is related to its role in proper sulfide detoxification in mitochondria, which is released by the enzyme activity of β-cyanoalanine synthase C1 (Garcia et al., 2010). The loss of a functional

OAS-C in the mitochondria causes phenotypic characteristics very similar to the loss of the CYS-C1 activity. The *oas-c* null allele is defective in root hair elongation, thus confirming the previous conclusion that OAS-C plays a significant role in root (Watanabe et al., 2008). These root phenotypic traits of the *oas-c* null mutant have not been previously observed, due to differences in growth conditions, such as the presence of sucrose in the culture media. It seems clear that the phenotypic differences of the *oas-c* null mutant are exacerbated in some culture conditions, where the mitochondria have a greater involvement in the overall plant metabolism. Thus, in the presence of sucrose, the carbohydrate can supply both energy and carbon skeletons for growth, changing the plant metabolism towards more anaerobic than aerobic. In any case, the genetic complementation eliminates the phenotypic differences of the *oas-c* mutants from wild type plants, thus demonstrating that the hair root defects is due to the disruption of the *OAS-C* gene.

Knocking out the *OAS-C* gene also compromises the performance of the mitochondrial respiration chain because the resulting sulfide during the cyanide detoxification cannot re-assimilate into cysteine. The presence of sulfide in mitochondria in as little as nanomolar concentrations would lead to inhibition of cytochrome c oxidase, similar to inhibition of this enzyme by cyanide (Nicholson et al., 1998; Dorman et al., 2002). It has been suggested that sulfide can reach the cytosol via diffusion through the chloroplast envelope membranes to serve as substrate for the bulk of Cys synthesis (Wirtz and Hell, 2007; Haas et al., 2008). Similarly, we can assume that the excess of sulfide could be diffused out of the mitochondria to be re-assimilated into cysteine in the cytosol. However, in metabolically active cells, protons are typically pumped out of the matrix and the pH of the mitochondrial stroma is therefore about 8, compared to the neutral pH (approximately 7) of the cytosol and intermembrane space. At this pH the sulfide is predominantly present in the charged HS^- form and the transport would be very limited (Lowicka and Beltowski, 2007). Consequently, the absence of a functional OAS-C provokes the accumulation of sulfide in the mitochondria at levels that are measurable in total tissue extracts by using an H_2S-selective electrode. In addition, a

decrease of both the *CYS-C1* gene expression level and total β-cyanoalanine synthase activity level in the oas-c null mutant to avoid also an over-accumulation of lethal cyanide amounts.

Moreover, the respiration rates measured in the *oas-c* null mutant show that oxygen consumption is induced in the leaves and even more strongly induced in the roots by an increase in the alternative oxidase pathway as demonstrated by the effect of SHAM on the respiration rates and by the increase of the *AOX1a* gene expression. Plant mitochondria possess two different pathways of electron transport at the ubiquinone level, the cyanide- and sulfide-sensitive cytochrome pathway and the cyanide-resistant alternative pathway. The alternative oxidase is responsible for the latter and is not coupled to ATP synthesis like in the cytochrome pathway (Vanlerberghe and McIntosh, 1997). One of the suggested biological functions of the alternative pathway is to reduce the formation of ROS because the mitochondrial electron transport chain produces significant quantities of ROS due to the presence of the ubisemiquinone radical. This radical can transfer a single electron to oxygen, generating superoxide. Thus, mechanisms that maintain the flow of electrons out of the ubiquinone pool reduce ROS production, such as is the case of the alternative pathway (Wagner and Krab, 1995; Purvis, 1997; Maxwell et al., 1999; Moller, 2001). Therefore, alternative respiration has been implicated in stress alleviation. However, it is evident that the induction of the alternative oxidase is not sufficient to reduce ROS generation as we observed leaf and root accumulation of H_2O_2 that induces cell death in the *oas-c* null mutant. The pattern of cell death as groups of dead cells observed in the *oas-c* mutant leaves is typically triggered by the perturbation of H_2O_2 homeostasis (Dat et al., 2003; Lopez-Martin et al., 2008).

The inability of the alternative oxidase to prevent the production of reactive oxygen species may be due to the accumulation of sulfide in addition to cyanide. The ability of thiols to promote iron-induced ROS generation is well known (Yang et al., 2000). Additionally, the toxicity of H_2S has been attributed to its ability to inhibit cytochrome c oxidase in a manner similar to HCN, although recently it has been proposed that the NaHS- induced ROS formation in a dose-dependent manner also

contributes to hydrogen sulfide toxicity. In mammalian systems, it has been suggested that a metal containing enzyme, such as P450, catalyses the auto-oxidation of H_2S for ROS formation (Eghbal et al., 2004; Truong et al., 2006). Similarly, this mechanism of ROS induction may be occurring in the *oas-c* null mutant, as demonstrated by our results.

A collateral finding of our work is to find that the splice variant 1 of the *OAS-C* gene does not appear functional. The disruption of variant 1 with the T-DNA insertion causes no phenotypic characteristics distinct from the wild type strain. Furthermore, the expression levels of variant 1 are not significant along the different growth stages (Supplementary Figure 2 online). Curiously, in a recent study using 2-D electrophoresis followed by ESI Q-TOF and MALDI-TOFF mass spectrometry, three different protein spots of OAS-C have been identified (Wirtz et al., 2010). Although alternative splicing products can generate different protein subspecies, it is very improbable that one of the OAS-C protein spots arise from variant 1, taking into consideration the high abundance of the protein spots. It is more plausible that the different spots were derived from different posttranscriptional modifications already described for other OASTL isoforms, such as N-terminal acetylation (Wirtz et al., 2010) and tyrosine-nitration (Alvarez et al., 2011). This latter modification has been recently described to strongly affect OASTL activity of the cytosolic OAS-A1 protein due to a drastically reduced capacity of the nitrated protein to bind the O-acetylserine substrate and to a reduced stabilisation of the pyridoxal-5′-phosphate cofactor through hydrogen bonds that is essential for full activity (Alvarez et al., 2011).

METHODS

Plant Material and Growth Conditions

The *Arabidopsis thaliana* wild type ecotype Col-0 and the T-DNA insertional mutants SALK_000860 and WiscDsLox381A8 were used in this work (Alonso et al.,

2003). Plant materials were obtained from the NASC (European Arabidopsis Stock Centre).

To generate the *SALK_00860* complementation line, the SSP Gateway Clone U25275 (Yamada et al., 2003) was obtained from the ABRC (Arabidopsis Biological Resource Center) containing the full-length coding sequence of *OAS-C* in the pENTR/D-TOPO vector. The cDNA fragment was then transferred into the pMDC32 vector (Curtis and Grossniklaus, 2003) using the Gateway system (Invitrogen) according to the manufacturer's instructions. The final construct was generated by transformation into *Agrobacterium tumefaciens* and then introduced into *SALK_00860* null plants using the floral-dip method (Clough and Bent, 1998).

The plants were grown either in soil irrigated with Hoagland II medium (Jones, 1982), or in solid one-half Murashige & Skoog medium or in solid one-half Murashige & Skoog containing one-fourth macronutrients in Petri dishes. When required, the medium was supplemented with 30 mg ml^{-1} kanamycin (for the SALK mutant) or 25 mg ml^{-1} Basta and 20 mg ml^{-1} hygromycin (for the Wisc mutant), or with 1% (w/v) sucrose. Plants were grown under a photoperiod of 16 h of white light (120 µE m^{-2} s^{-1}) at 20ºC and 8 h dark at 18ºC.

RNA Isolation and Real-time RT-PCR

Total RNA was extracted from *Arabidopsis* leaves using the RNeasy Plant Mini Kit (Qiagen) and retro-transcribed using oligo(dT) primer and the Superscript™ First-Strand Synthesis System for RT-PCR (Invitrogen). Gene-specific primers for each gene were designed using the Vector NTI Advance 10 software (Invitrogen) (Supplementary Table 1 online). The PCR efficiency of all primer pairs was determined to be 100%. Real-time PCR reactions were performed using iQ™ SYBR Green Supermix (Bio-Rad); the signals were detected on an iCYCLER (Bio-Rad) according to the manufacturer's instructions. The cycling parameters consisted of 95°C for 10 min, 45 cycles of 95°C for 15 s and 60°C for 1 min. A melt curve from 60°C to 90°C was run following the PCR cycling. The expression level of the genes of interest was normalised to that of the constitutive *UBQ10* gene by subtracting the

CT value of *UBQ10* from the CT value of the gene (ΔCT) and calculated as $2^{-(\Delta CT)}$. The expression relative to the wild type level was calculated as $2^{-(\Delta CT \text{ mutant} - \Delta CT \text{ wild type})}$. The results shown are mean values ± SD of at least three independent RNA samples.

Determination of CAS Activity

CAS activity was measured by the release of sulfide from L-cysteine and cyanide using the method previously described (Burandt et al., 2002). Protein extracts were prepared by grinding the tissues in liquid nitrogen, extracting with 20 mM Tris-HCl, pH 9.0, and centrifugation at 13000 *g*, the resulting supernatant being the source of enzyme. The reaction mixture contained 100 mM Tris-HCl, pH 9.0, 0.8 mM L-cysteine, 10 mM KCN and 50-100 μl of protein extract. The reaction was initiated by the addition of L-Cys, incubated for 15 min at 30ºC and stopped with 30 mM $FeCl_3$ in 1.2 N HCl plus 20 mM N,N-dimethyl-p-phenylenediamine dihydrochloride in 7.2 N HCl. The formation of methylene blue was determined at 670 nm and using an extinction coefficient of $15x10^6$ cm^2 mol^{-1}. Total protein was quantified using the Bradford method (Bradford, 1976).

Quantification of Thiol Compounds

To quantify the total Cys and glutathione contents, thiols were extracted, reduced with $NaBH_4$, and quantified by reverse-phase HPLC after derivatization with monobromobimane (Molecular Probes) as previously described (Dominguez-Solis et al., 2001). Plant tissues were homogenized in cold extraction buffer (4 ml g^{-1} FW) containing 0.1 N HCl and 1 mM EDTA using a mortar and pestle with liquid nitrogen. Homogenates were centrifuged at 15000 *g* for 15 min in the cold. Thiols were reduced at 4 °C for 15 min by mixing 400 μl of extracted samples with 600 μl of 200 mM CHES, pH 9.2 and 100 μl of 250 mM $NaBH_4$. A 330-μl aliquot was derivatized in the dark for 15 min by adding 20 μl of 15 mM monobromobimane. The reaction was stopped by adding 250 μl of 0.25% (v/v) methanesulfonic acid at room temperature. Derivatized thiols were separated and quantified by reverse-phase

HPLC.

Measurements of Endogenous H_2S

Leaves (200 mg) were ground in liquid nitrogen to a fine powder and suspended in 150 μL of antioxidant buffer (62.5 g L^{-1} of sodium salicylate, 16.25 g L^{-1} of ascorbic acid and 21.25 g L^{-1} sodium ascorbate). After vortexing for 1 min and centrifugation at 15,000*g* for 15 min at 4ºC, H_2S was measured for 20 min at 25ºC in the resulting supernatant using a Micro Sulfide Ion Electrode (LIS-146AGSCM; Lazar Research Lab. Inc.). Concentrations of H_2S were determined from a calibration curve made with increasing concentrations of HNaS in antioxidant buffer. Each measurement was repeated twice, and data are indicated as the means ± SD for at least three independent biological experiments.

Cyanide Determination

Cyanide measurements were performed by HPLC as previously described (Garcia et al., 2010). Plant tissues were homogenized with liquid nitrogen and resuspended in cold borate-phosphate extraction buffer (2 ml g^{-1} FW) containing 27 mM sodium borate and 47 mM potassium phosphate, pH 8.0. Homogenates were centrifuged at 15000 *g* for 15 min in the cold. Extracted cyanide was subsequently quantified by reverse-phase HPLC after derivatization with NDA to form a CBI derivative. A cyanide standard solution (CertiPUR, Merck) was used to make a 6-point calibration curve over the concentration range of 0 to 3.8 mM. HPLC analyses were performed on a LaChrom Elite® system (VWR International, Darmstadt, Germany). The CBI derivative was separated on an RP 18 (150 mm × 3.9 mm, 5 μm; Waters, Germany) column. The mobile phase consisted of a mixture of acetonitrile and 0.1% trifluoracetic acid in water (28:72 v/v) and was delivered isocratically at a flow rate of 1 ml min^{-1}. The percentage of cyanide recovery using the described method was previously calculated as 69% (Garcia et al., 2010).

Detection and Quantification of Hydrogen Peroxide

For the histochemical detection of H_2O_2, mature leaves were immersed in 1 mg ml^{-1} DAB (Sigma-Aldrich), fixed with a solution of 3:1:1 (v/v/v) ethanol:lactic acid:glycerol and photographed. The quantification of H_2O_2 was performed following the protocol previously described (Joo et al., 2005). Basically, frozen plant tissue was hand ground in liquid nitrogen, and immediately resuspended in 10 mM Tris-HCl buffer, pH 7.5. The extract was centrifuged twice at 15,000 *g* for 10 min. We performed each measurement on two equal aliquots; one of which we added 100 mM ascorbate, and they were allowed to react for 15 min. Then ROS levels were assayed by adding H_2DCFDA in DMSO to both aliquots to a final concentration of 25 μM and incubating at 30ºC for 30 min. Fluorescence was measured using a Cary Eclipse fluorescence spectrophotometer (Varian, Inc.) with excitation/emission wavelengths set to 485 and 525 nm, respectively. We then subtracted the ascorbate insensitive background from each experimental value. Total protein was quantified using the Bradford method (Bradford, 1976). The average fluorescence value obtained from three successive measurements was divided by the protein content and expressed as relative fluorescence units per milligram of protein.

Detection of Cell Death

Trypan blue (Sigma-Aldrich) staining for dead cells in the leaves was performed by incubating the leaves in a lactic acid-phenol-trypan blue solution (2.5 mg ml^{-1} trypan blue, 25% [w/v] lactic acid, 23% phenol, 25% glycerol), then heating over boiling water for 1 min and finally destaining using a 2.5 g ml^{-1} chloral hydrate solution before photographing the leaves.

Respiration Measurements

Wild type and mutant plants were grown for 15 days on vertical MS-plates. Around 50 mg of separated leaves and root tissues were cut, dried on paper towels and transferred into airtight cuvettes containing 20 mM Hepes, pH 7.2 and 0.2 mM $CaCl_2$, and oxygen uptake was measured as a decrease in O_2 concentration in the dark using a Clark-type electrode. Cyanide-resistant O_2 uptake was measured in the presence of

0.5 mM KCN. The respiration component due to the alternative oxidase pathway was measured in the presence of 4 mM of the inhibitor SHAM. The results were expressed as the mean ± SD from at least three replica samples, and the experiment was repeated three times using independent samples.

Supplementary Data

Supplementary Figure 1 online. Phenotypes of the *oas-c* mutants in the presence of sucrose.

Supplementary Figure 2 online. Expression levels of the three *OAS-C* gene models in different tissues at different growth stages of *A. thaliana* plants.

Supplementary Table 1 online. Oligonucleotides used in this work

ACKNOWLEDGMENTS

This work was funded in part by the European Regional Development Fund (ERDF) through the Ministerio de Ciencia e Innovación (grant no. BIO2010-15201) and the Junta de Andalucía (grant nos. BIO–273). This work was also funded by the CONSOLIDER CSD2007–00057, Spain, and by JAE program (CSIC) to C.A. for fellowship support. We thank Inmaculada Moreno for technical help with the research work.

FIGURE LEGENDS

Figure 1. Enzymatic reactions involved in cyanide detoxification in *A. thaliana* mitochondria.

The CAS enzyme CYS-C1 catalyses the conversion of cyanide plus cysteine to form β-cyanoalanine (CN-ALA) plus sulfide, which is used by the OASTL enzyme OAS-C to incorporate it to O-acetylserine (OAS) to form cysteine.

Figure 2. Identification of *OAS-C* tagged T-DNA mutants.

(A) Intron-exon organization of the three *OAS-C* gene models and location of the T-DNA insertion in the SALK_000860 and WiscDsLox381A8 insertion mutants. The 3'-end has been magnified to show the location and direction of the primers used for the mutant analysis: qOAS-CF1 (F1), qOAS-CR1 (R1), qOAS-CF2-3 (F2-3) and qOAS-CR2-3 (R2-3). **(B)** Real-time RT-PCR analysis of the SALK_000860 and WiscDsLox381A8 mutant plants. RNA samples were prepared from the leaves of wild type, SALK_000860 and WiscDsLox381A8 mutant plants, and the primers specific for the *OAS-C* gene (pairs *F1/R1* for variant 1 and *F2-3/R2-3* for variants 2 and 3) and for the constitutive *UBQ10* (*qUBQ10F/ qUBQ10R*) transcripts were used. The transcript levels were normalized to the constitutive *UBQ10* gene. Data shown are means $\pm$ SD of three independent experiments. ND: non-detected.

Figure 3. Relative expression level of the OASTL gene family in the SALK_000860 mutant plant.

Real-time RT-PCR analysis of the expression of the *OAS-A1 (At4g14880), OAS-B (At2g43750), DES1 (At5g28030), CS26 (At3g03630), CYS-C1 (At3g61440), CYS-D1 (At3g04940)*, and *CYS-D2 (At5g28020)* genes was performed in the leaves and roots from the wild type and the SALK_000860 mutant plants grown for three weeks under control conditions. The transcript levels were normalized to the constitutive *UBQ10* gene. Data shown are means $\pm$ SD of three independent experiments, and

they represent the transcript level of each gene in the mutant plants relative to the transcript level in the wild type plants. ANOVA was performed using the software OriginPro 8. *, $P < 0.05$

Figure 4. Root phenotypes of the *oas-c* mutants.
Representative bright field images of roots from wild type, SALK_000860 and WiscDsLox381A8 insertion mutants and the SALK_00860 complementation line seedlings, growing for eight days on MS medium without sucrose. Two different roots from different batches of seedlings are shown for each line.

Figure 5. Whole seedling phenotypes of the *oas-c* mutants.
Representative bright field images of eight-day-old wild type, SALK_000860 and WiscDsLox381A8 insertion mutants and the SALK_00860 complementation line seedlings, growing on MS medium with one-fourth of macronutrients without sucrose. Two different batches of seedlings are shown.

Figure 6. Relative expression level of the alternative oxidase gene *AOX1a* in the *oas-c* mutants.
Real-time RT-PCR analysis of the expression of the *AOX1a (At3g22370)* gene was performed in the leaves from 15-day-old wild type and the *oas-c* mutants. The transcript levels were normalized to the constitutive *UBQ10* gene. Data shown are means $\pm$ SD of three independent experiments and they represent the transcript level of each gene in the mutant plants relative to the transcript level in the wild type plants. ANOVA was performed using the software OriginPro 8. *, $P < 0.05$.

Figure 7. Respiration rates in the leaves and roots of the *oas-c* mutants.
The respiration rate was measured in the leaf and root tissues of 15-days-old wild type and the *oas-c* mutant plant lines with an oxygen electrode. Alternative oxidase respiration was determined in the presence of 4 mM SHAM. The results were expressed as the mean $\pm$ SD of three independent analyses. ANOVA was performed

using the software OriginPro 8. Significant differences between wild type and mutant plants in different conditions are indicated with one asterisk ($P < 0.05$).

Figure 8. Accumulation of H_2O_2 and lesion formation in the *oas-c* mutants.
(A) Histochemical detection of H_2O_2 in detached leaves from three-week-old plants by DAB staining. The experiment was repeated at least three times with similar results. **(B)** Quantification of H_2O_2 in root tissues from three-week-old wild type and mutant plants by H_2DCFDA fluorescence as described in methods. The results were expressed as the mean $\pm$ SD of three independent analyses. ANOVA was performed using the software OriginPro 8. *, $P < 0.05$. **(C)** Spontaneous cell death detection in detached leaves from three-week-old plants by trypan blue staining. The insert shows a magnified photo of a lesion in the leaf from SALK_000860 mutant plant. The experiment was repeated at least three times with similar results.

Table 1. Thiol content of the *oas-c* mutants.

Plant line	Total Cys (nmol g^{-1} FW)		Total Glutathione (nmol g^{-1} FW)	
	Leaves	Roots	Leaves	Roots
Wt	26.97 ± 1.49	65.41 ± 4.14	307.3 ± 8.1	201.2 ± 4.1
SALK_000860	28.41 ± 1.12	46.37 ± 2.24 *	328.9 ± 3.8	144.2 ± 7.5*
WiscDsLox381A8	25.65 ± 0.98	60.19 ± 4.05	312.5 ± 3.8	185.3 ± 20.6

Total levels of Cys and glutathione were measured in the leaves and roots of wild type and *oas-c* mutant plants grown for three weeks in soil. Values are means ± SD of three independent experiments. ANOVA was performed using the software OriginPro 8. *, $P < 0.05$.

Table 2. CAS activity and cyanide and sulfide contents in the *oas-c* mutants.

Plant line	CAS activity (nmol min^{-1} mg^{-1})		CN content (nmol g^{-1}FW)		Sulfide content (nmol g^{-1}FW)	
	Leaves	Roots	Leaves	Roots	Leaves	Roots
Wt	3.50 ± 0.26	11.05 ± 0.57	0.80 + 0.02	4.14 ± 0.11	12.18 + 1.48	2.10 + 0.33
SALK_000860	2.97 ± 0.25	7.75 ± 0.23*	0.86 ± 0.03	5.18 ± 0.18*	21.50 + 0.94*	4.35 + 0.13*
WiscDsLox381A8	3.65 ± 0.17	11.25 ± 0.55	0.76 ± 0.03	4.28 ± 0.22	11.80 + 1.28	2.01 + 0.69

CAS enzyme activity and total levels of sulfide and cyanide were measured in the leaves and roots of wild type and *oas-c* mutant plants grown for three weeks in soil. Values are means ± SD of three independent experiments. ANOVA was performed using the software OriginPro 8. *, $P < 0.05$.

REFERENCES

Alonso, J.M., et al. (2003). Genome-wide insertional mutagenesis of Arabidopsis thaliana. Science. **301,** 653-657.

Alvarez, C., Calo, L., Romero, L.C., Garcia, I., and Gotor, C. (2010). An O-acetylserine(thiol)lyase homolog with L-cysteine desulfhydrase activity regulates cysteine homeostasis in Arabidopsis. Plant Physiol. **152,** 656-669.

Alvarez, C., Lozano-Juste, J., Romero, L.C., Garcia, I., Gotor, C., and Leon, J. (2011). Inhibition of Arabidopsis O-acetylserine(thiol)lyase A1 by tyrosine nitration. J. Biol. Chem. **286,** 578-586.

Bermudez, M.A., Paez-Ochoa, M.A., Gotor, C., and Romero, L.C. (2010). Arabidopsis S-sulfocysteine synthase activity is essential for chloroplast function and long-day light-dependent redox control. Plant Cell. **22,** 403-416.

Bleecker, A.B., and Kende, H. (2000). Ethylene: a gaseous signal molecule in plants. Annu. Rev. Cell. Dev. Biol. **16,** 1-18.

Bottcher, C., Westphal, L., Schmotz, C., Prade, E., Scheel, D., and Glawischnig, E. (2009). The multifunctional enzyme CYP71B15 (PHYTOALEXIN DEFICIENT3) converts cysteine-indole-3-acetonitrile to camalexin in the indole-3-acetonitrile metabolic network of Arabidopsis thaliana. Plant Cell. **21,** 1830-1845.

Bradford, M.M. (1976). A rapid and sensitive method for the quantitation of microgram quantities of protein utilizing the principle of protein-dye binding. Anal. Biochem.**72,** 248-254.

Burandt, P., Schmidt, A., and Papenbrock, J. (2002). Three O-acetyl-L-serine(thiol)lyase isoenzymes from Arabidopsis catalyse cysteine synthesis and cysteine desulfuration at different pH values. J. Plant Physiol. **159,** 111-119.

Cooper, C.E., and Brown, G.C. (2008). The inhibition of mitochondrial cytochrome oxidase by the gases carbon monoxide, nitric oxide, hydrogen cyanide and hydrogen sulfide: chemical mechanism and physiological significance. J. Bioenerg. Biomembr. **40,** 533-539.

Curtis, M.D., and Grossniklaus, U. (2003). A gateway cloning vector set for high-throughput functional analysis of genes in planta. Plant Physiol. **133,** 462-469.

Dat, J.F., Pellinen, R., Beeckman, T., Van De Cotte, B., Langebartels, C., Kangasjarvi, J., Inze, D., and Van Breusegem, F. (2003). Changes in hydrogen peroxide homeostasis trigger an active cell death process in tobacco. Plant J. **33,** 621-632.

Dominguez-Solis, J.R., Gutierrez-Alcala, G., Vega, J.M., Romero, L.C., and Gotor, C. (2001). The cytosolic O-acetylserine(thiol)lyase gene is regulated by heavy metals and can function in cadmium tolerance. J. Biol. Chem. **276,** 9297-9302.

Dorman, D.C., Moulin, F.J., McManus, B.E., Mahle, K.C., James, R.A., and Struve, M.F. (2002). Cytochrome oxidase inhibition induced by acute hydrogen sulfide inhalation: correlation with tissue sulfide concentrations in the rat brain, liver, lung, and nasal epithelium. Toxicol. Sci. **65,** 18-25.

Eghbal, M.A., Pennefather, P.S., and O'Brien, P.J. (2004). H2S cytotoxicity mechanism involves reactive oxygen species formation and mitochondrial depolarisation. Toxicology. **203,** 69-76.

Garcia, I., Castellano, J.M., Vioque, B., Solano, R., Gotor, C., and Romero, L.C. (2010). Mitochondrial {beta}-Cyanoalanine Synthase Is Essential for Root Hair Formation in Arabidopsis thaliana. Plant Cell. **22,** 3268-3279.

Haas, F.H., Heeg, C., Queiroz, R., Bauer, A., Wirtz, M., and Hell, R. (2008). Mitochondrial serine acetyltransferase functions as a pacemaker of cysteine synthesis in plant cells. Plant Physiol. **148,** 1055-1067.

Hatzfeld, Y., Maruyama, A., Schmidt, A., Noji, M., Ishizawa, K., and Saito, K. (2000). beta-Cyanoalanine synthase is a mitochondrial cysteine synthase-like protein in spinach and Arabidopsis. Plant Physiol. **123,** 1163-1171.

Heeg, C., Kruse, C., Jost, R., Gutensohn, M., Ruppert, T., Wirtz, M., and Hell, R. (2008). Analysis of the Arabidopsis O-acetylserine(thiol)lyase gene family demonstrates compartment-specific differences in the regulation of cysteine synthesis. Plant Cell. **20,** 168-185.

Jones, J.B. (1982). Hydroponics: its history and use in plant nutrition studies. J. Plant Nut. **5,** 1003-1030.

Joo, J.H., Wang, S., Chen, J.G., Jones, A.M., and Fedoroff, N.V. (2005). Different signaling and cell death roles of heterotrimeric G protein alpha and beta subunits in the Arabidopsis oxidative stress response to ozone. Plant Cell. **17,** 957-970.

Jost, R., Berkowitz, O., Wirtz, M., Hopkins, L., Hawkesford, M.J., and Hell, R. (2000). Genomic and functional characterization of the oas gene family encoding O-acetylserine (thiol) lyases, enzymes catalyzing the final step in cysteine biosynthesis in Arabidopsis thaliana. Gene. **253,** 237-247.

Krueger, S., Niehl, A., Lopez Martin, M.C., Steinhauser, D., Donath, A., Hildebrandt, T., Romero, L.C., Hoefgen, R., Gotor, C., and Hesse, H. (2009). Analysis of cytosolic and plastidic serine acetyltransferase mutants and subcellular metabolite distributions suggests interplay of the cellular compartments for cysteine biosynthesis in Arabidopsis. Plant Cell Environ. **32,** 349-367.

Lopez-Martin, M.C., Becana, M., Romero, L.C., and Gotor, C. (2008). Knocking out cytosolic cysteine synthesis compromises the antioxidant capacity of

the cytosol to maintain discrete concentrations of hydrogen peroxide in Arabidopsis. Plant Physiol. **147,** 562-572.

Lowicka, E., and Beltowski, J. (2007). Hydrogen sulfide (H2S) - the third gas of interest for pharmacologists. Pharmacol. Rep. **59,** 4-24.

Maxwell, D.P., Wang, Y., and McIntosh, L. (1999). The alternative oxidase lowers mitochondrial reactive oxygen production in plant cells. Proc. Nat. Acad. Sci. USA **96,** 8271-8276.

Moller, I.M. (2001). PLANT MITOCHONDRIA AND OXIDATIVE STRESS: Electron Transport, NADPH Turnover, and Metabolism of Reactive Oxygen Species. Annu. Rev. Plant Physiol. Plant Mol. Biol. **52,** 561-591.

Nakamura, T., Yamaguchi, Y., and Sano, H. (2000). Plant mercaptopyruvate sulfurtransferases - Molecular cloning, subcellular localization and enzymatic activities. Eur. J. Biochem.**267,** 5621-5630.

Nicholson, R.A., Roth, S.H., Zhang, A., Zheng, J., Brookes, J., Skrajny, B., and Bennington, R. (1998). Inhibition of respiratory and bioenergetic mechanisms by hydrogen sulfide in mammalian brain. J. Toxicol. Environ. Health A. **54,** 491-507.

Papenbrock, J., and Schmidt, A. (2000). Characterization of two sulfurtransferase isozymes from Arabidopsis thaliana. Eur. J. Biochem. **267,** 5571-5579.

Papenbrock, J., Guretzki, S., and Henne, M. (2011). Latest news about the sulfurtransferase protein family of higher plants. Amino Acids. 41**,** 43-57.

Peiser, G.D., Wang, T.T., Hoffman, N.E., Yang, S.F., Liu, H.W., and Walsh, C.T. (1984). Formation of cyanide from carbon 1 of 1-aminocyclopropane-1-carboxylic acid during its conversion to ethylene. Proc. Nat. Acad. Sci. USA. **81,** 3059-3063.

Piotrowski, M. (2008). Primary or secondary? Versatile nitrilases in plant metabolism. Phytochemistry. **69,** 2655-2667.

Purvis, A.C. (1997). Role of the alternative oxidase in limiting superoxide production by plant mitochondria. Physiol. Plant. **100,** 165-170.

Siegien, I., and Bogatek, R. (2006). Cyanide action in plants - from toxic to regulatory. Acta Physiol. Plant. **28,** 483-497.

Truong, D.H., Eghbal, M.A., Hindmarsh, W., Roth, S.H., and O'Brien, P.J. (2006). Molecular mechanisms of hydrogen sulfide toxicity. Drug Metab. Rev. **38,** 733-744.

Vanlerberghe, G.C., and McIntosh, L. (1997). ALTERNATIVE OXIDASE: From Gene to Function. Annu. Rev. Plant Physiol. Plant Mol. Biol. **48,** 703-734.

Wagner, A.M., and Krab, K. (1995). THE ALTERNATIVE RESPIRATION PATHWAY IN PLANTS - ROLE AND REGULATION. Physiol. Plant. **95,** 318-325.

Watanabe, M., Kusano, M., Oikawa, A., Fukushima, A., Noji, M., and Saito, K. (2008). Physiological roles of the beta-substituted alanine synthase gene family in Arabidopsis. Plant Physiol. **146,** 310-320.

Watanabe, M., Kusano, M., Oikawa, A., Fukushima, A., Noji, M., and Saito, K. (2008a). Physiological roles of the beta-substituted alanine synthase gene family in Arabidopsis. Plant Physiol. **146,** 310-320.

Watanabe, M., Mochida, K., Kato, T., Tabata, S., Yoshimoto, N., Noji, M., and Saito, K. (2008b). Comparative genomics and reverse genetics analysis reveal indispensable functions of the serine acetyltransferase gene family in Arabidopsis. Plant Cell. **20,** 2484-2496.

Wirtz, M., and Hell, R. (2007). Dominant-negative modification reveals the regulatory function of the multimeric cysteine synthase protein complex in transgenic tobacco. Plant Cell. **19,** 625-639.

Wirtz, M., Heeg, C., Samami, A.A., Ruppert, T., and Hell, R. (2010). Enzymes of cysteine synthesis show extensive and conserved modifications patterns that include N(alpha)-terminal acetylation. Amino Acids. **39,** 1077-1086.

Yamada, K., et al. (2003). Empirical analysis of transcriptional activity in the Arabidopsis genome. Science. **302,** 842-846.

Yamaguchi, Y., Nakamura, T., Kusano, T., and Sano, H. (2000). Three Arabidopsis genes encoding proteins with differential activities for cysteine synthase and beta-cyanoalanine synthase. Plant Cell Physiol. **41,** 465-476.

Yang, E.Y., Campbell, A., and Bondy, S.C. (2000). Configuration of thiols dictates their ability to promote iron-induced reactive oxygen species generation. Redox Rep. **5,** 371-375.

Figure 1

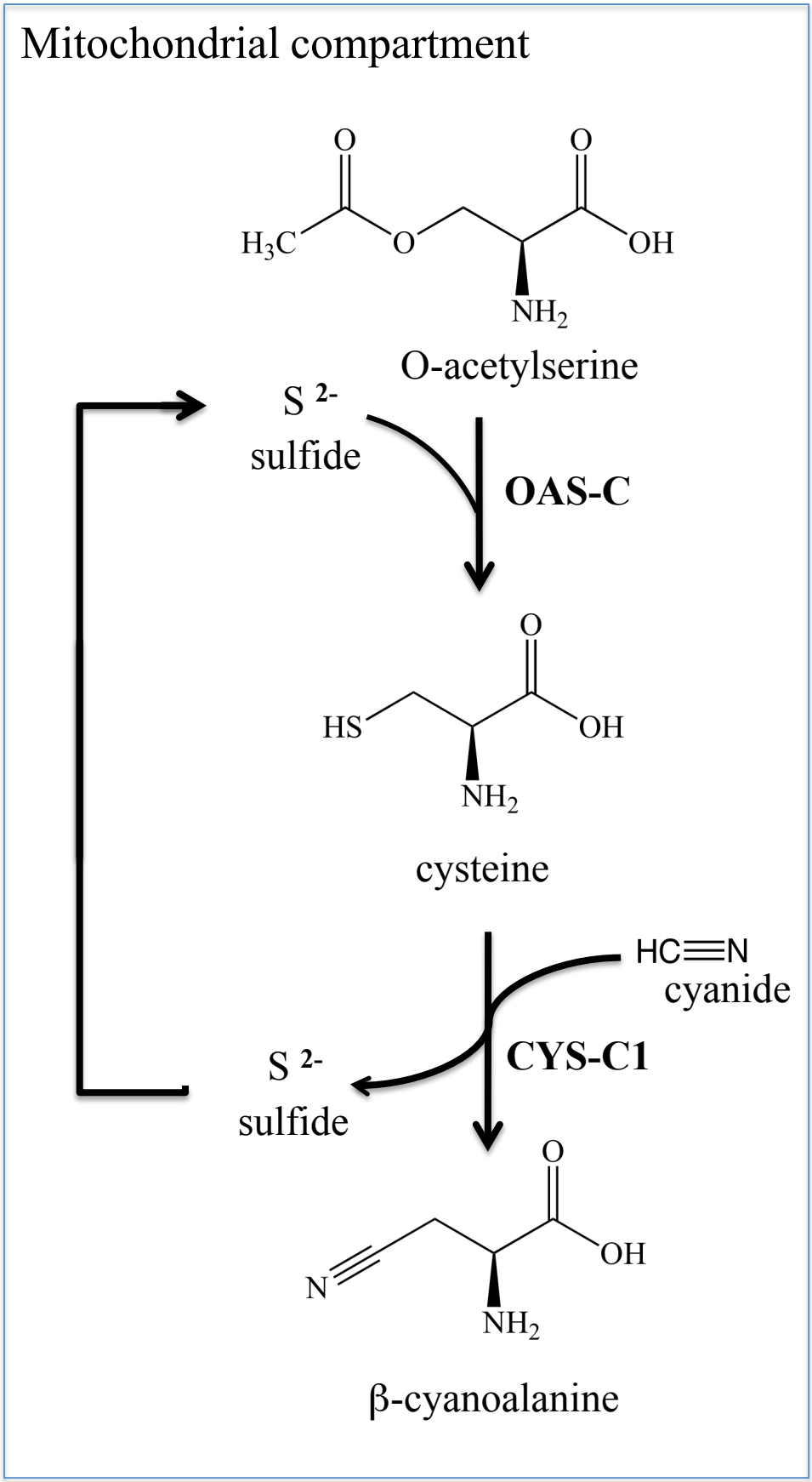
Mitochondrial compartment
O
O
H3C
O
OH
NH2
O-acetylserine
S 2-
sulfide
OAS-C
O
HS
OH
NH2
cysteine
HC≡N
cyanide
CYS-C1
S 2-
sulfide
O
N
OH
NH2
β-cyanoalanine

Figure 2

(A)

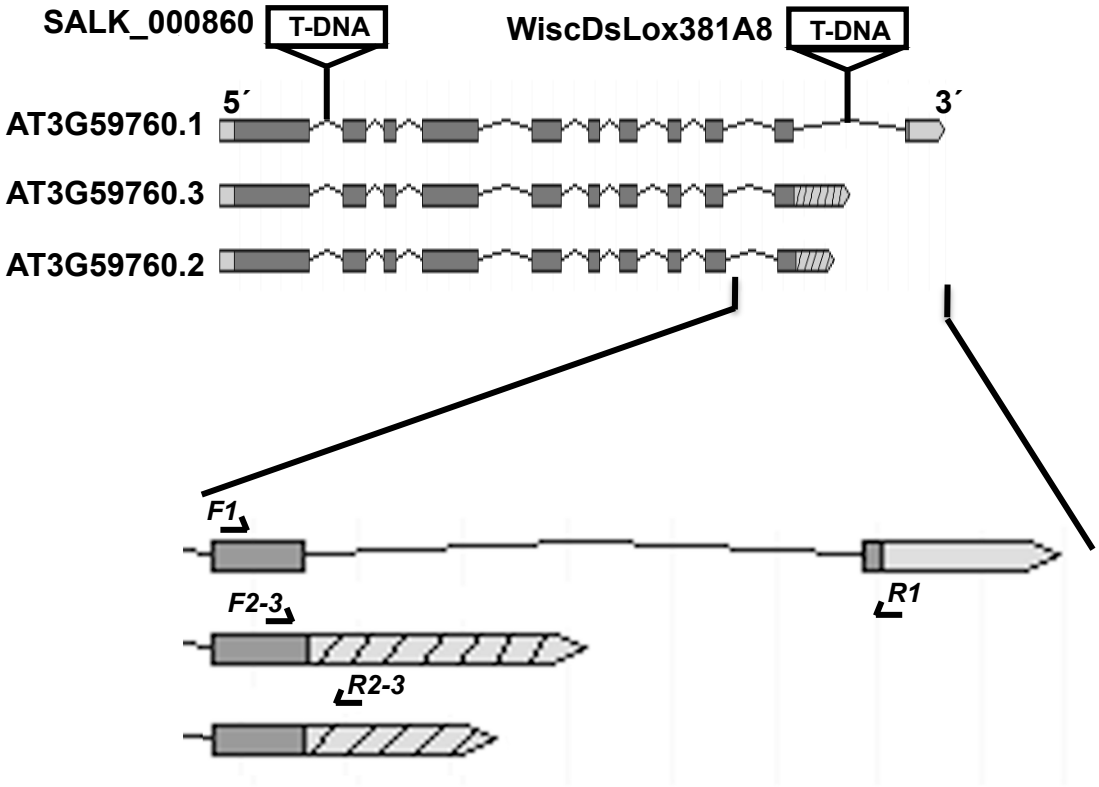

(B)

Plant line	Expression levels	
	Gene models 2 and 3	Gene model 1
Wt	0.15 ± 0.024	0.0001± 0.00002
SALK_000860	ND	ND
WiscDsLox381A8	0.13 ± 0.012	ND

Figure 3

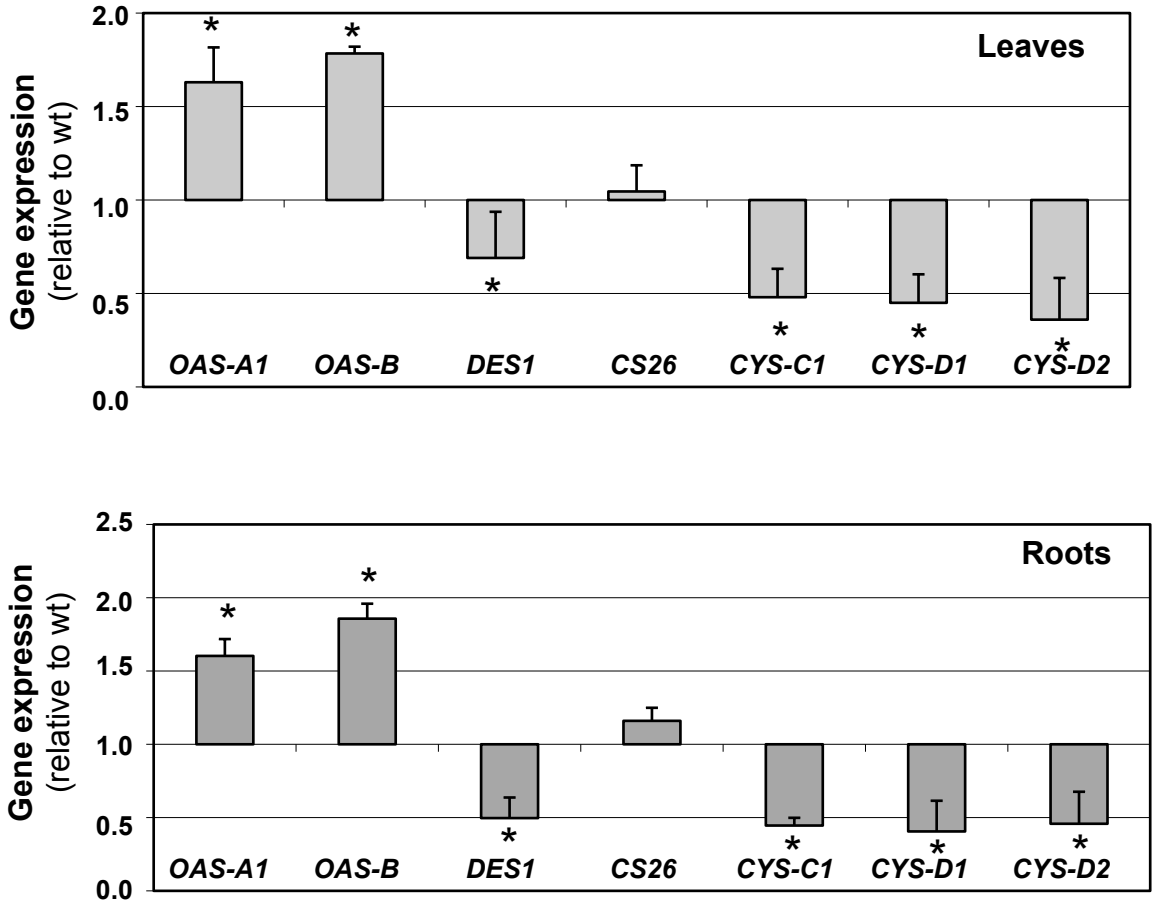
Leaves
Gene expression
(relative to wt)
2.0
1.5
1.0
0.5
0.0
OAS-A1
OAS-B
DES1
CS26
CYS-C1
CYS-D1
CYS-D2
Roots
Gene expression
(relative to wt)
2.5
2.0
1.5
1.0
0.5
0.0
OAS-A1
OAS-B
DES1
CS26
CYS-C1
CYS-D1
CYS-D2

Figure 4

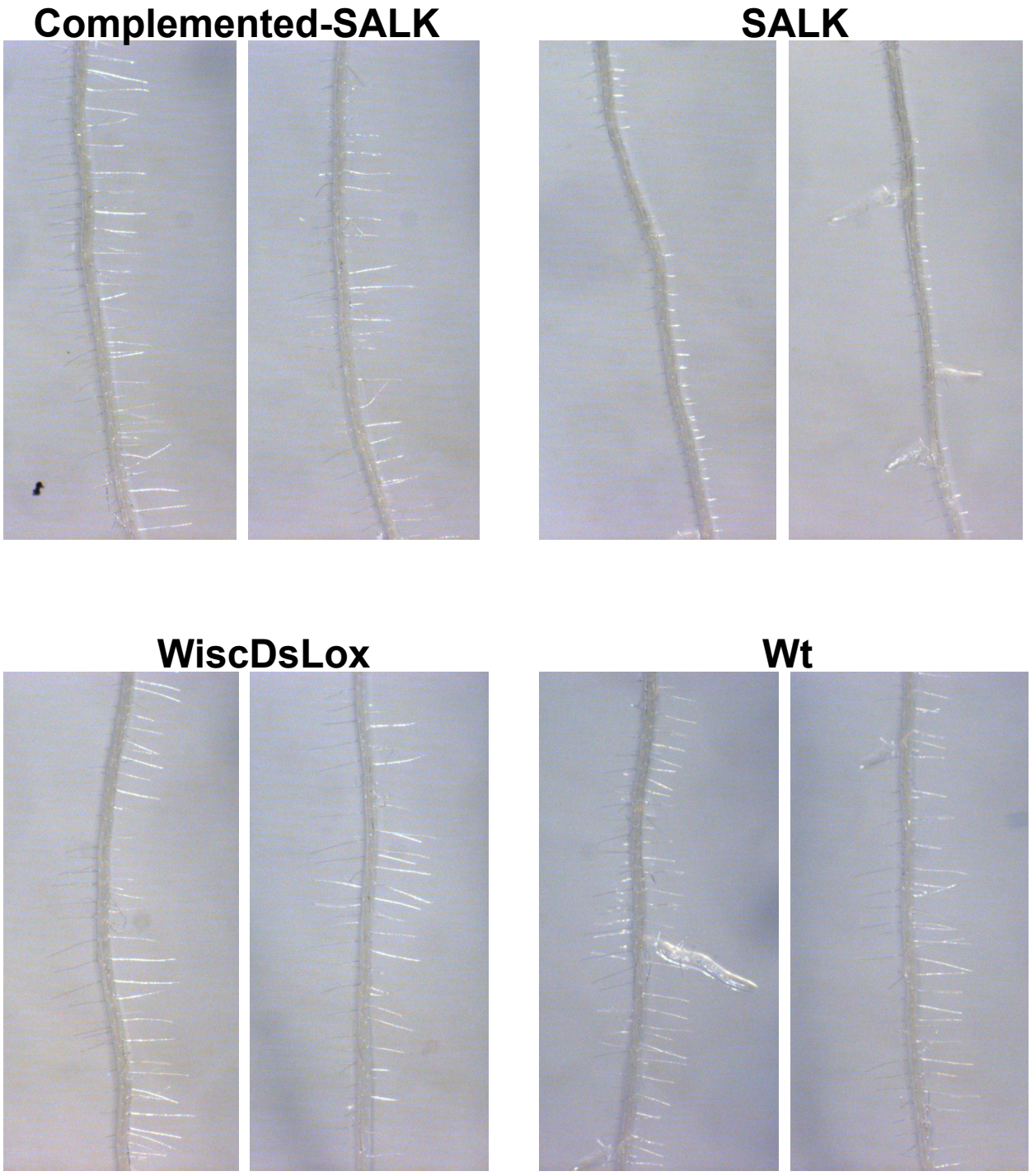

Figure 5

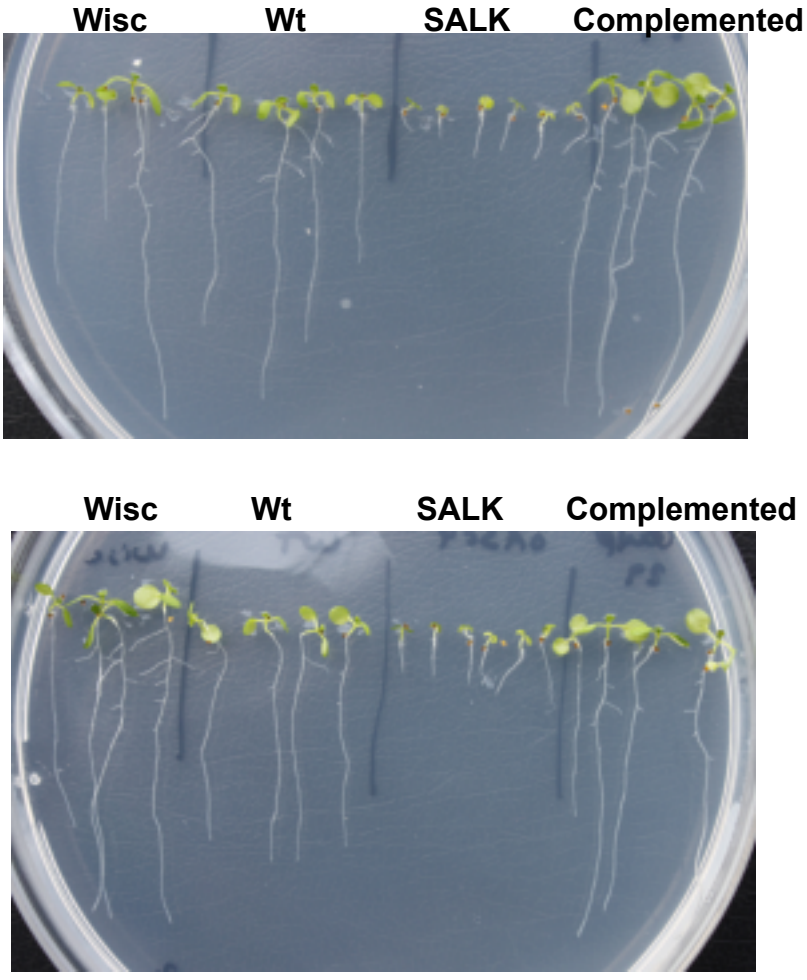

Figure 6

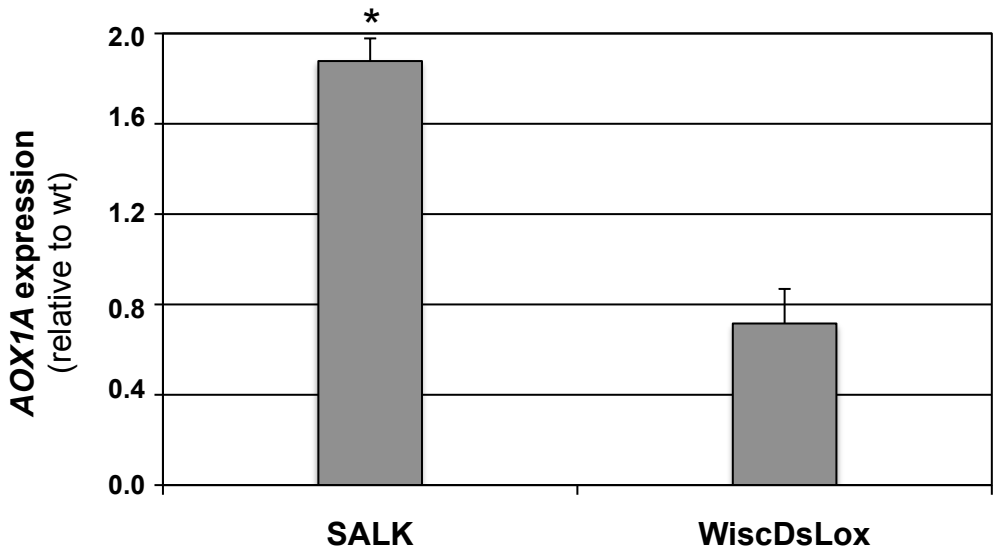
*
2.0
1.6
1.2
0.8
0.4
0.0
AOX1A expression
(relative to wt)
SALK
WiscDsLox

Figure 7

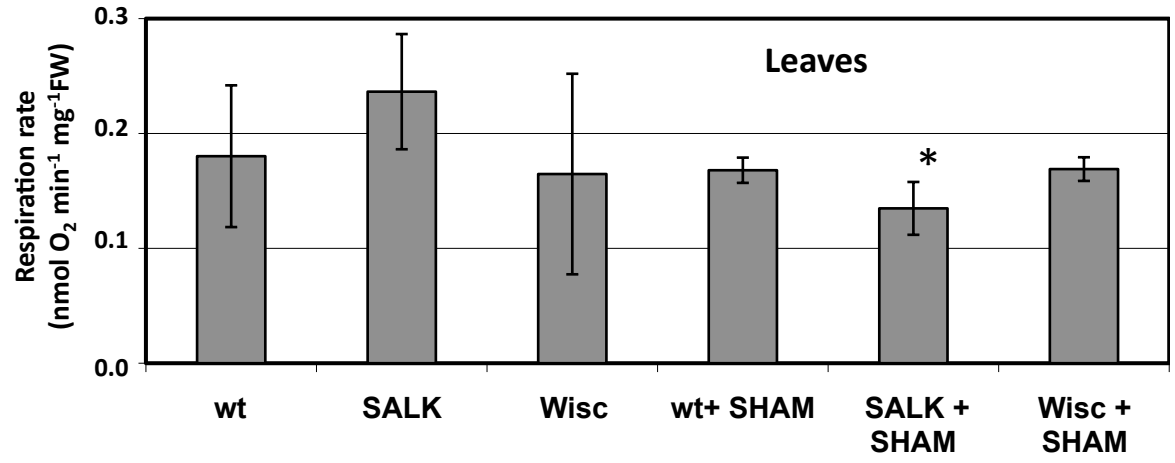
Leaves
Respiration rate
(nmol O_2 min^{-1} $mg^{-1}FW$)
0.3
0.2
0.1
0.0
*
wt
SALK
Wisc
wt+ SHAM
SALK + SHAM
Wisc + SHAM

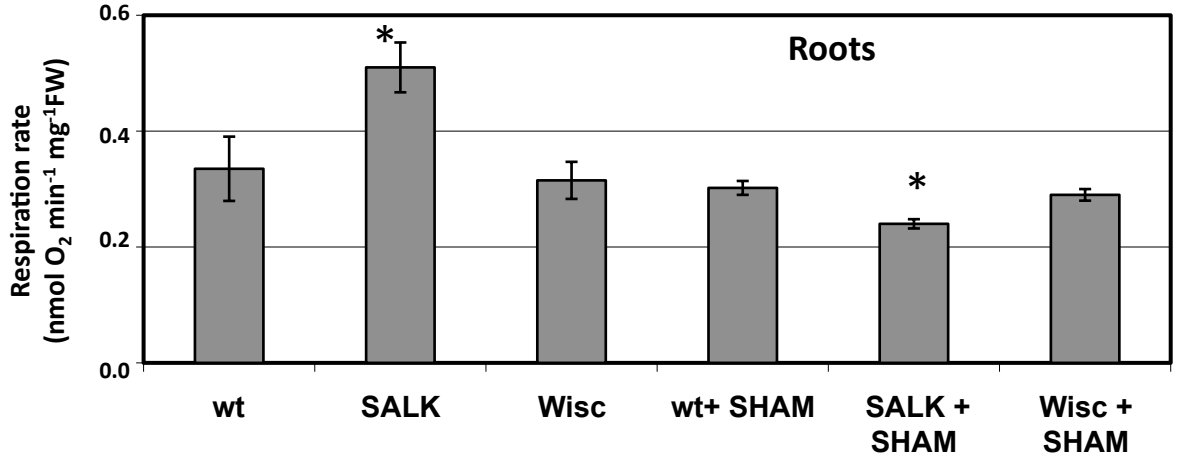
Roots
Respiration rate
(nmol O_2 min^{-1} $mg^{-1}FW$)
0.6
0.4
0.2
0.0
*
*
wt
SALK
Wisc
wt+ SHAM
SALK + SHAM
Wisc + SHAM

Figure 8

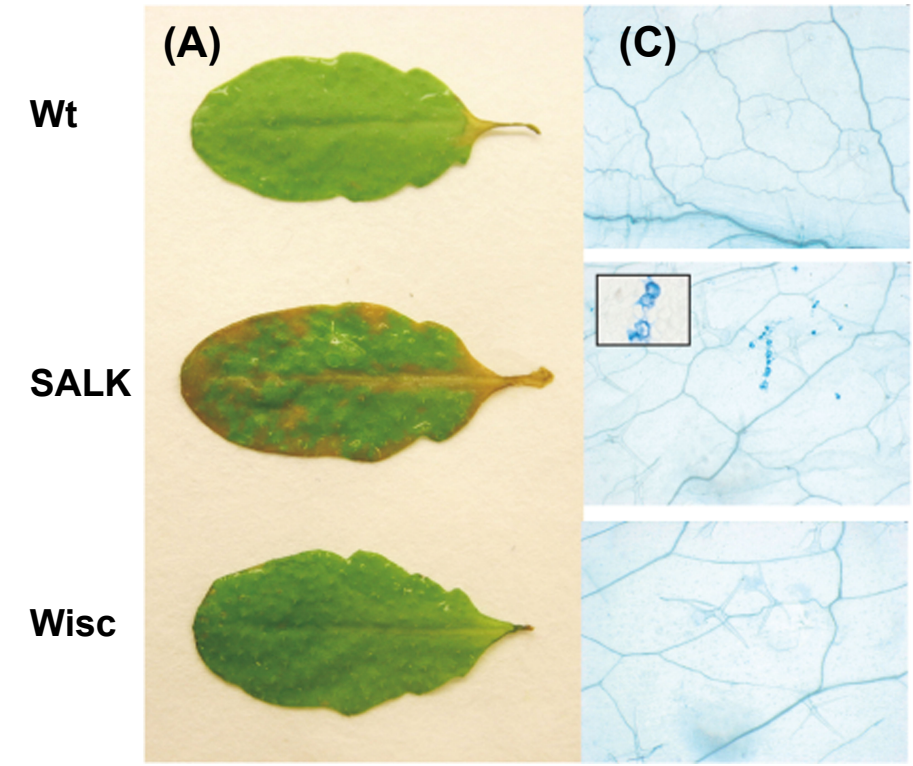
(A)
(C)
Wt
SALK
Wisc

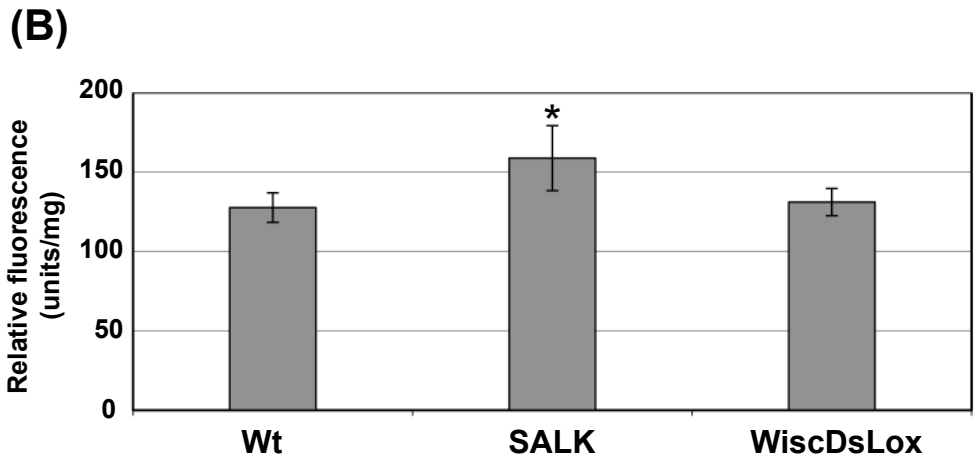
(B)
Relative fluorescence (units/mg)
200
150
100
50
0
*
Wt
SALK
WiscDsLox